Developing a monitoring system for Toyota Prius battery-packs for longer term performance issues

Peter Leijen
AECS Ltd.
897 Valley Road
Hastings, New Zealand
peter@aecs.net

Nihal Kularatna
School of Engineering
The University of Waikato
Hamilton, New Zealand
nihalkul@waikato.ac.nz

***Abstract*—The Toyota Prius battery pack consists of 38 individual battery blades, each blade contains 6 NiMH cells in series. This means that each pack contains 228 NiMH cells. Given this number of individually manufactured cells combined into a large battery pack, any individual cell or a blade getting weaker than all other linearly degrading cells, will become the performance limiting element in the pack. For example in a situation where one blade weakens down to 1200mAh compared to all other 37 blades maintaining approximately 2400mAh capacity will make the car run only 1.3 km in EV mode, compared to 2.6 km if all 38 blades are of 2400mAh capacity. In order to identify such individually weak cells, a supercapacitor based monitoring system is designed and the paper indicates the approach in developing this system, together with some details explaining the general performance of the overall system and how the new monitoring system can help in managing the battery pack life issues in the Toyota Prius.**

Keywords - Electric Vehicles, Supercapacitors, Battery Management

I. INTRODUCTION

The most difficult issue in developing electric vehicles (EV) and hybrid electric vehicles (HEV) is to get the optimally performing large capacity battery packs with suitable battery management systems (BMS). Over the past two decades there has been a lot of research and development on the battery packs, drive trains and optimization applicable to these areas [1]. Toyota Prius is a car which has come into the HEV market within the last decade and it has a battery pack based on 228 NiMH cells, organized into blades of 6 series connected cells. The Toyota Prius system is complex and contains a number of technically advanced systems that make diagnostics both interesting and difficult. The apparent ground loop though the converter assembly to the middle of the battery pack results in high voltages across the battery pack. The battery management electronic control unit (ECU) of the Toyota Prius measures various battery-related parameters including temperature, voltage and current. When one of these parameters falls outside of predetermined levels a diagnostic trouble code (DTC) is logged. The quality of the battery pack determines the fuel efficiency of the vehicle. Swings in battery voltage indicate to the BMS when to start and stop charging with the internal combustion engine (ICE). Battery quality can be defined as its capacity or state of health [2]. There are many different methods of measuring state of health (SOH) and state of charge (SOC) as outlined in [2]–[7]. The easiest method of measuring blade capacity is Coulomb counting, a simple integral of current over time [8]. Battery SOH is more difficult to measure as we also need to take into account other failure methods such as short-circuited cells, etc [8]. Ref [9] details a method for measuring the SOH and the capacity of Prius battery packs. A major concern to Prius owners is the lifetime of their battery pack. Toyota states that the battery pack will last 160,000 km or ten years. However as per the experience of companies such as AECS where this research work is ongoing, Prius battery packs have failed prematurely. This paper investigates the effects of a reduced-capacity blade, and the effects of a blade with very poor SOH, on the performance of the battery pack. The paper also details a simple battery model used to describe the behaviour of the battery blades under different conditions and proposes a monitoring system for early detection and prevention of battery failure, based on a supercapacitor bank based sub-system.

II. TOYOTA PRIUS SYSTEM

The battery pack of the Toyota Prius consists of 38 NiMH blades (Figure 1) each of which contain six NiMH cells in series [10]. Toyota has designed their system to operate in a split battery fashion, i.e. the apparent ground (chassis) of the HV battery pack occurs between blades 19 and 20, where the service plug is fitted. The battery management system of the Prius (Figure 1) does several sub tasks:

- It takes a differential voltage measurement across each pair of blades,
- Total current into the pack is measured,
- Four temperature measurements are performed throughout the whole pack.

Each pair of battery blades will be referred to as a battery block in this paper.

The diagram in figure 1 does not show how the inverter/converter assembly links the battery management ECU, the battery pack and the auxiliary power source (12 V battery). The inverter converts the DC battery voltage to a pseudo three-phase sinusoidal waveform using 6 duty-cycle controlled switches (IGBTs). The three-phase voltage is used to drive the motor-generator set and is the main source of propulsion. Belt-driven components such as the power steering pump, air-conditioning compressor and the alternator have been removed from the ICE to further improve the fuel efficiency. The power steering hydraulics are driven by an electronic pump. Similarly

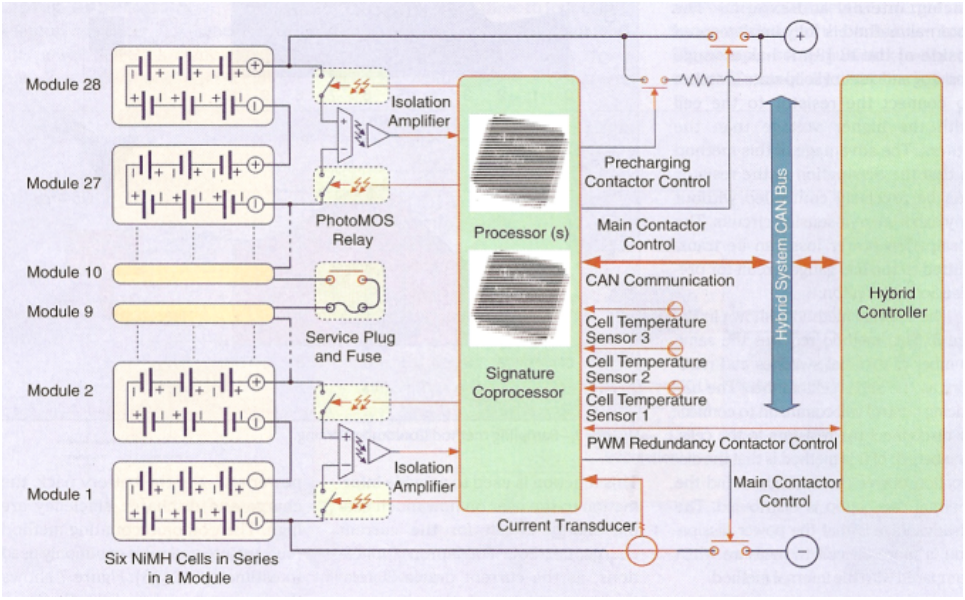

Fig. 1. A typical Battery Management System for HEVs- 2009 Toyota Prius BMS. [11]

the air-conditioning compressor has also been changed. The alternator has been replaced by a DC-DC converter.

III. TOYOTA PRIUS BMS BATTERY-RELATED FAULT CODES

The Toyota Prius battery management system (BMS) monitors battery temperature and battery voltage with the sensors explained in section II. If any of the voltages or temperatures of the battery blocks fall outside of predetermined trigger levels for a prolonged period of time the BMS will log the malfunction and store a diagnostic trouble code (DTC). The vehicle will then enter a so-called "turtle" mode when a code is set. Turtle mode is equivalent to limp-home mode in a conventional vehicle. In this state of operation the vehicle has reduced power output. For HEVs this means that the current drawn from the battery, and charging current, are limited resulting in poor fuel economy, and make the vehicle almost undrivable. Two of the most common battery-related DTCs are "Leak Detected" and "Battery Block Malfunction". The work detailed in this paper was focused on the causes for the "Battery Block Malfunction" fault code, and early detection/monitoring system.

A. Battery Block Malfunction Condition

The Battery Block Malfunction DTC (DTC number P3011 to P3029) is triggered by cells that have poor state of health. The battery management ECU looks at the voltage difference between individual battery blocks under charge and discharge. A voltage difference of less than 0.3 V is acceptable (Figure 2) according to Toyota repair advice [12]. This measurement technique is essentially a method for measuring the overall impedance of the battery block. Battery impedance is also related to the state of health of the cell [6], [7]. A cell with higher AC or DC impedance, higher voltage difference, is deemed to be of lesser SOH. This method also measures relative SoC between the battery blocks. The voltage of the block with less SoC will collapse before that of a cell with higher SoC.

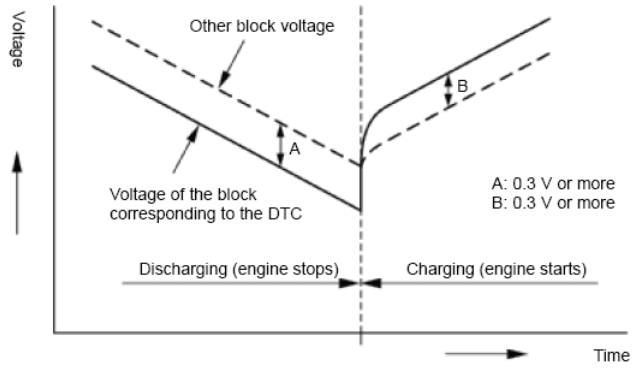

Fig. 2. Voltage difference while charging and discharging [12].

Another method of diagnosing this DTC, suggested by Toyota, is to look at the swing between the maximum and the minimum block voltages, as shown in Figure 3. The maximum allowable voltage swing is 2 V.

As mentioned above, this DTC is produced due to mismatching of battery blades within the battery pack. Replacing the complete battery pack assembly is one possible fix to this problem. However this repair cost, in the order of several thousands of dollars can be prohibitive, particularly for a car used for several years. However, compared to this single blade faulty condition, there is a large range of battery configurations and battery SOH distributions which will not generate a fault code. Next sections discuss the implications of such battery arrangements and outline a proposed monitoring system to identify these individual situations.

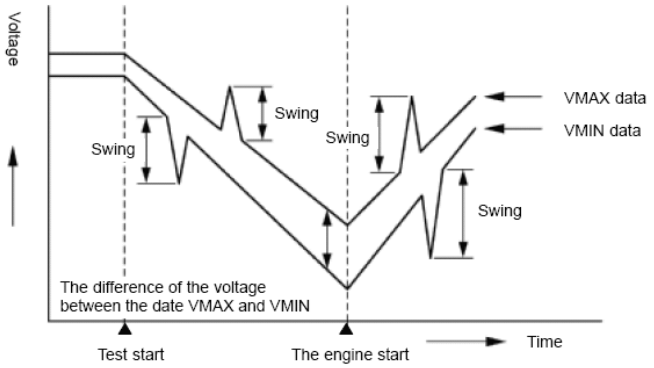

Fig. 3. Voltage swing between maximum block voltage and minimum block voltage while charging and discharging [12].

IV. CURRENT ISSUE

When a large number of series connected cells are exposed to high charge and discharge rates under slightly varying conditions, some cells could easily degrade in a non-linear fashion. Figure 4 shows the non-linear fashion in which four different battery packs have deteriorated over time. These battery packs were analyzed in the lab to find the capacity distribution and steady state voltages of the individual battery blades. Known broken and poor state of health cells were then substituted into a good battery pack and road-tested in a Toyota Prius (Model: NHW11, Engine Type: 1FX, Year: 2001), to investigate the failure methods of the battery packs.

V. CAPACITY DISTRIBUTION

Figure 4 shows the measured capacities per battery blade, using a coulomb counting algorithm between end of discharge and end of charge points. Both Packs 2 and 3 have aged in a similar fashion where the blades near the ends of the packs have higher capacities than the blades in the middle but are otherwise uniform. The "bathtub" curve appears to be due to the temperature differences throughout the pack during normal operation.

1) Effect of one reduced capacity blade within a pack : It was determined that Pack 3 was of good health because the pack performed the same as the original Prius battery pack. Cell #38 (Cell ID 01M) from Pack 3 was replaced with cell #38 (Cell ID 41D) from Pack 2. The battery characteristics are summarized in Table I Cell 41D was chosen to have approximately half the capacity of rest of the pack with a similar steady state voltage.

TABLE I. CELLS REPLACED WITHIN BATTERY PACK.

Cell ID	Capacity	Steady Voltage
01M	2482.2 mAh	7.81 V
41D	1164.4 mAh	7.55 V

With the Battery Pack 3 in the vehicle it was able to drive 2.6 km in EV mode. When one blade was replaced with a blade of approximately half its capacity as shown in Table I the vehicle was only able to travel 1.3 km in EV mode. No fault code was triggered with this cell arrangement even though the fuel efficiency of the vehicle was halved. This test confirmed that the battery pack was only as good as its weakest blade and that matching state of health (of each blade) and balancing the state of charge in one battery pack is vital to the performance and fuel efficiency of the vehicle.

VI. PROPOSED MONITORING SYSTEM

The Toyota Prius battery pack is a large series connected bank of batteries in the order of 280-300 V at an average capacity of 1500-2000 mAh as per the results in Figure 4. In order to achieve an optimum driving range and performance from the battery pack, the pack requires periodic monitoring of each blade and individually balancing each blade. Market research has shown that people who drive EV or HEVs adhere to a regular service schedule maintaining items such as brake pads, engine fluids etc. However, nobody considers (or advised of) performing battery maintenance. The slow degradation of the battery pack over time means that many serious battery blade mismatches go unnoticed. The proposed monitoring system connects to the existing vehicle wiring loom (without any modifications to the base system) and performs a series of charge and discharge tests to determine individual SOH/ SOC for each pair of blades. A simple model is used to describe the battery blades, resulting in Equation (1) based on testing for high frequency, low frequency and steady state responses of the battery blade. This equation however doesnt include a temperature component which has a large effect on the battery performance. Figure 5 shows how the capacities of two battery blades vary with temperature.

In order to achieve the results as per Figure 5 a Coulomb count was performed between end-of-discharge and end-of-charge points, while the battery blade was at a controlled temperature using a temperature controlled chamber. The battery blade temperature was controlled by placing it in a temperature controlled chamber and allowing 24 hours for cell temperature to stabilize before the test was started. The tests were repeated three times for common environmental temperatures (within a range of 15 to 25°C) to ensure that an accurate relationship can be formed in this temperature range. The results show that the measured battery capacity increases with temperature. Testing also showed that the variation in open circuit terminal voltage of the battery decreased by 0.9 mV per degree temperature rise. It can therefore be concluded that the variation in capacity is not attributed to by a variation in terminal voltage but purely caused by changes in the chemical acceptance of the electrolyte [13] [14].

$$V_t(I_{load}) = 1.255 \times \left(\text{SOC}_0 - \frac{\int I_{load}\, dt}{\text{capacity(SOH)}}\right) - RI_{load} - L\frac{dI_{load}}{dt} + 7.145 \quad (1)$$

$$V_{oc}(\text{SOC}) = 1.255 \times \text{SOC} + 7.145 \qquad 0.3 < \text{SOC} < 0.7 \quad (2)$$

Monitoring of the battery voltage during discharge is required to detect faulty or short-circuited cells within a battery blade. The energy removed from a battery blade during this discharge stage is temporarily stored in a super-capacitor bank

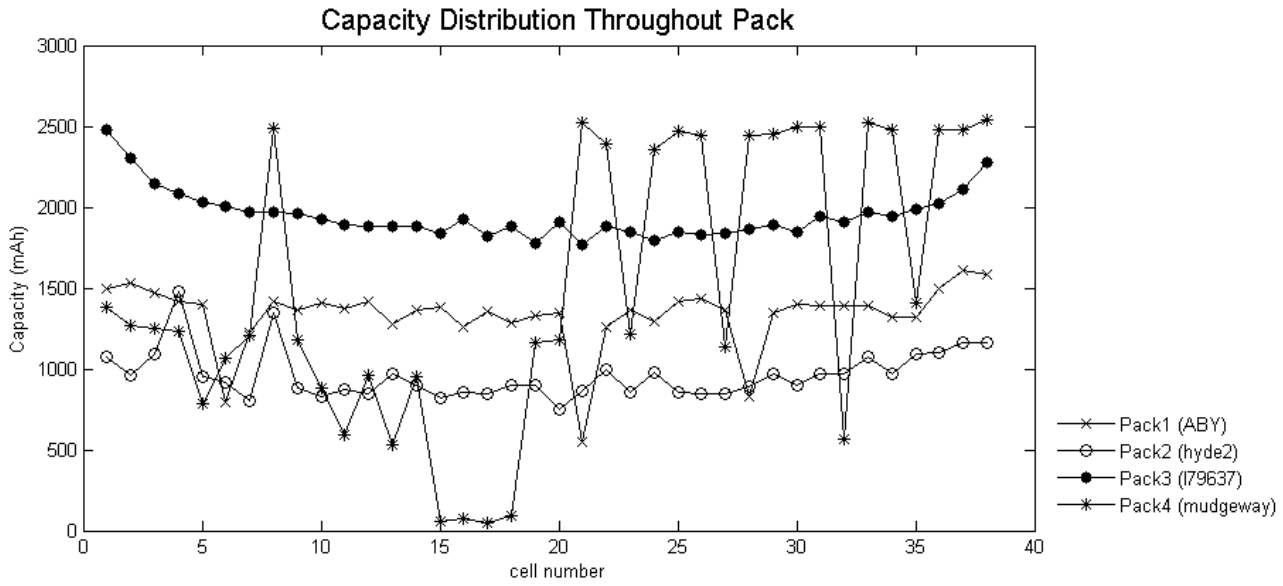

Fig. 4. Capacity Distribution throughout four packs tested.

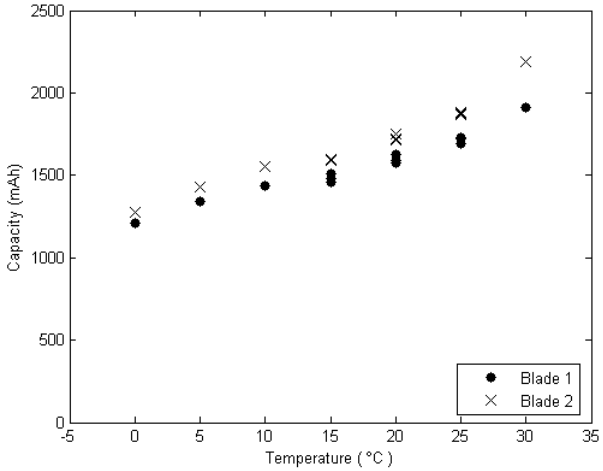

Fig. 5. Battery Blade capacity variation with temperature.

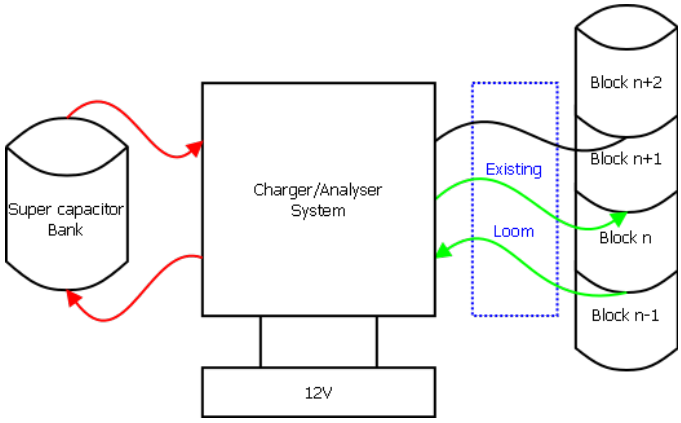

Fig. 6. Discharge Block n into super-capacitor bank.

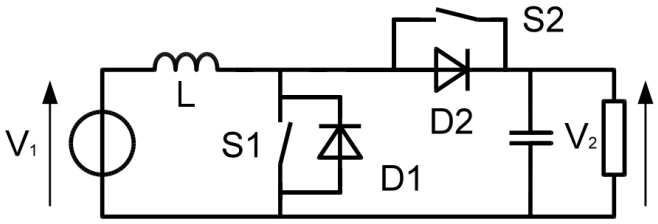

Fig. 7. Bi-Directional Buck-Boost power supply assuming ideal components.

and transferred to next battery blade in the pack through a series of switches and associated circuitry. Figure 6 shows the discharge phase of the analysis process and how the various components of the proposed system are arranged.

The charger/analyser system consists of a bi-directional buck-boost circuit shown in Figure 7. This circuit allows for efficient conversion of energy from the higher voltage battery block to the lower voltage capacitor bank and visa-versa. The circuit shows that the super-capacitor bank (V1) must always be of a lower voltage than the battery block (V2) otherwise diode D2 will become forward biased and effectively short circuit the super-capacitor bank.

Energy is effectively recycled throughout the analysis process as one battery block is discharged into another battery block isolated through the use of a super-capacitor bank. The battery voltage is analysed during the discharge phase and the current is integrated (Coulomb count) during the charge phase. The near linear relationship between battery state of charge and battery voltage shown in Figure 8 and Equation (2) makes it possible to determine battery state of health by charging the battery by only a small percentage and analysing the voltage difference. The result of the current integral then corresponds to a fixed SoC. The current integral can then be multiplied by the appropriate factor to calculate SOH or capacity of the cell.

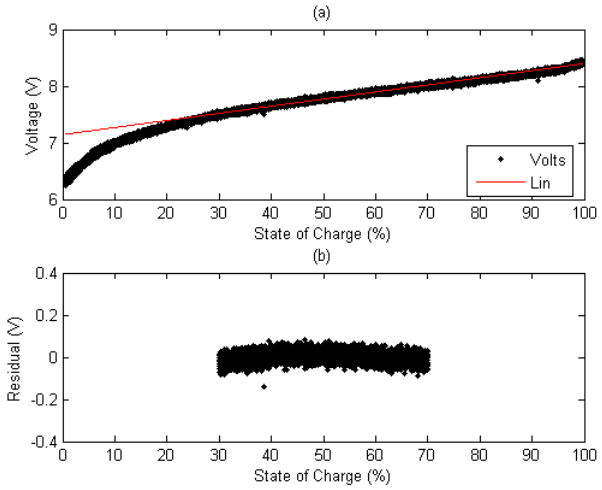

Fig. 8. (a) Linear fit to the discharge S-curve (b) plot of residuals for the linear fit.

Equation (2) describes the linear fit shown in Figure 8.

2) Application of Battery Model: The battery model shown in equation 2 shows a direct linear relationship between state of charge and open circuit voltage between 30 and 70 percent state of charge. Therefore $\Delta V_{OC} \propto \Delta\text{SOC}$ and $\Delta\text{SOC} = \int I_{load}\, dt$. Combining these two values allows calculation of overall capacity (SOH).

A. Use of Supercapacitors

Figure 9 shows a size comparison of three energy storage devices and the Table II compares the energy storage capabilities of the three components. The AA battery stores the largest amount of energy. However the AA battery also has very high internal resistance compared to the capacitors. This means that the charge and discharge efficiency of the battery is very low [15]. The battery also has a low terminal voltage. The supercapacitor and the electrolytic capacitor (Panasonic) store very similar amounts of energy however the Panasonic capacitor needs to be charged to 450 V whereas the super-capacitor has a terminal voltage of only 2.5 V for the same amount of energy. A typical battery blade's terminal voltage varies from 6.2 V (end of discharge) to 8.4 V end of charge. The super-capacitor bank needs to cover twice this range of voltages to be able to efficiently cycle energy from one battery block (pair of blades) to another battery block.

TABLE II. ENERGY STORAGE COMPARISON

Component	Value	Voltage	Energy
Panasonic Capacitor	3300 μF,	450 V	$E_c = \frac{1}{2}C \times V^2$ = **334 J**
Super-Capacitor	110 F	2.5 V	$E_c = \frac{1}{2}C \times V^2$ = **343 J**
AA battery	2500 mAh, 9000 As	1.2 V	$E_b = As \times V$ = **10800 J**

A 10 V capacitor bank is used in the proposed design. The 10 V bank consists of 8 super-capacitors arranged in such a manner that there are two parallel banks of 10 V. A novel series-parallel switch allows the capacitor bank to be switched from a 10 V parallel arrangement to a 20 V series arrangement.

Fig. 9. Size comparison (a) capacitor from Prius inverter (b) PowerStor Aerogel super-capacitor (c) Energizer AA battery.

Figure 10 shows how the efficiency of the buck stage of the Bi-Direction Buck-Boost converter changes as the super-capacitor bank is charged. Fundamental equations can be applied to the circuit to calculate the efficiency of the converter at different conditions.

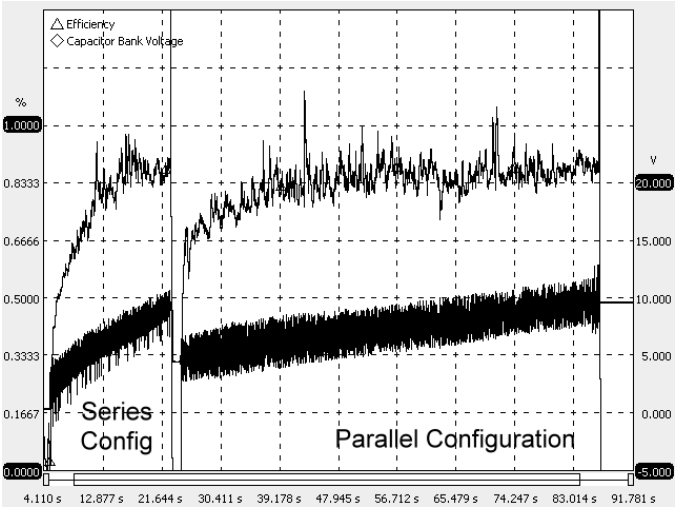

Fig. 10. Scope trace showing converter efficiency and super-capacitor voltage when the capacitors are in a series configuration and parallel configuration.

Switching the capacitors in such a manner also allows the maximum amount of energy to be extracted from the capacitor bank as it discharges. A super-capacitor bank was chosen for use in the proposed monitoring system because of their low

internal resistance and very good reversible energy storage characteristics which means that they are able to withstand many charge discharge cycles at high charge/discharge rates [16].

VII. SUMMARY OF BATTERY PACK PERFORMANCE AND ACHIEVEMENTS

Many battery pack failures are caused by a single battery blade or block failing as shown in Figure 4. Figure 4 shows that the capacities of the blades within the pack either decrease in a linear and very consistent manner, exemplified by Pack 1 and Pack 2, or the battery blade capacities decrease unpredictably as observed in the Pack 1 (ABY) and Pack4 (mudgeway) battery packs. Pack I79637 is still of good health, indicated by its relatively high average capacity. Pack2 (hyde2) is of poor health, evidenced by its low capacity. The capacities in Pack1 have decreased linearly only three blades have significantly less capacity and one battery blade has poor state of health, resulting in poor fuel economy. Field data collected has proven the concept that a battery pack from a vehicle which presented a "Battery Block Malfunction" fault code has been successfully rebuilt by finding and replacing the faulty battery blades with matched battery blades from a different pack. The vehicles useful life has been increased by reconditioning the battery pack.

VIII. FUTURE IMPROVEMENTS

It was found during testing that the parameters of the battery model vary with temperature indicating a stepped change between 10 and 15°C. These parameters need to be quantified and included in the initial battery model.

IX. CONCLUSION

The research so far has lead to developing a simplified battery model which accurately describes the behaviour of the "blade" under different conditions. Suitable circuitry has been developed to handle the power conversion between series connected battery blocks through an existing wiring loom using a super-capacitor bank as an isolating and energy-transfer medium. Various sensors have been interfaced with appropriate control circuitry and switch gear.

ACKNOWLEDGMENT

Authors would like to thank Toyota New Zealand for providing Prius battery packs for analysis, Paul Hyde from Hyde Automotive for the battery packs provided, and Mudgeway for their battery pack and associated parts which were used during the experiments. We would also like to thank AECS Ltd for providing valuable assistance with the interpretation of the large amount of test data and the use of their test equipment.

REFERENCES

[1] M. Eshani, Y. Gao, and A. Emadi, "Modern electric, hybrid electric and fuel cell vehicles," *CRC Press*, p. 534, September 2010.

[2] G. L. Plett, "Recursive approximate weighted total least squares estimation of battery cell total capacity," *Journal of Power Sources*, vol. 196, no. 4, pp. 2319–2331, 2011.

[3] H. Li, C. Liao, and L. Wang, "Research on state-of-charge estimation of battery pack used on hybrid electric vehicle," *IEEE*, 2009, hard copy.

[4] W. Guoliang, L. Rengui, Z. Chunbo, and C. Chan, "State of charge estimation for nimh battery based on electromotive force method," *IEEE Vehicle Power and Propulsion Conference*, no. 3-5, 2008.

[5] K. Bundy, M. Karlsson, G. Lindbergh, and A. Lundqvist, "An electrochemical impedance spectroscopy method for prediction of the state of charge of a nickel-metal hydride battery at open circuit and during discharge," *Journal of Power Sources*, vol. 72, no. 2, pp. 118–125, 1998.

[6] I. Buchmann, *Batteries in a Portable World*, second edition ed., C. E. Inc., Ed. Cadex Electronics Inc., 2001.

[7] L. Zhang, "Ac impedance studies on sealed nickel metal hydride batteries over cycle life in analog and digital operations," *Electrochimica Acta*, vol. 43, no. 21-22, pp. 3333–3342, 1998.

[8] P. Leijen and J. Scott, "Failure analysis of some toyota prius battery packs and potential for recovery," 2011. [Online]. Available: www.pjmldesign.co.nz

[9] P. Leijen, "Off-line nimh battery state of charge and state of health measurement," 2011. [Online]. Available: www.pjmldesign.co.nz

[10] W. K. Hu, M. M. Geng, X. P. Gao, T. Burchardt, Z. X. Gong, D. Norus, and N. K. Nakstad, "Effect of long-term overcharge and operated temperature on performance of rechargeable nimh cells," *Journal of Power Sources*, vol. 159, no. 2, pp. 1478–1483, 2006.

[11] J. Cao and A. Emadi, "Batteries need electronics," *IEEE Industrial Electronics*, vol. 5, no. 1, 2011.

[12] Toyota, *Toyota Prius Workshop manual*, 2001.

[13] E. L. Schneider, W. Kindlein Jr, S. Souza, and C. F. Malfatti, "Assessment and reuse of secondary batteries cells," *Journal of Power Sources*, vol. 189, no. 2, pp. 1264–1269, 2009.

[14] D. Linden and T. B. Reddy, *Handbook of Batteries*, third edition ed. McGraw-Hill, 1995.

[15] Maxwell. (2012) datasheet_k2_series. [Online]. Available: http://www.maxwell.com/

[16] P. Sharma and T. Bhatti, "A review on electrochemical double-layer capacitors," *Energy Conversion and Management*, vol. 51, pp. 2901–2912, 2010.